Atila SKANDARNEZHAD[1], Abdolreza RAHMATI[1], Adib ABRISHAMIFAR[1], Sina SHAHMOHAMMADI[1]

Faculty of Electrical Engineering, Iran University of Science and Technology, Tehran, Iran (1)

doi:10.15199/48.2015.10.27

Critical Current Control (C^3) and Modelling of a Buck Based LED Driver with Power Factor Correction

Abstract. *Buck converter has a good aptitude for LED driver application. Here a new technique introduced to control and model a buck converter in the closed loop condition using Lagrange equation. To improve the final model accuracy, parasitic elements of the converter are taken into account. The main advantage of this method is its novelty and simple implementation. Also, the converter power factor has improved under critical current control (C^3) technique. Frequency response and step response of the small signal model are derived and analysed. The theoretical predictions are tested and validated by means of PSIM software. Finally, precise agreement between the proposed model and the simulation results has obtained.*

Streszczenie. *IW artykule analizowano zastosowanie przekształtnika typu buck do zasilania diod LED. Zaproponowano nowy układ z uwzględnieniem elementów zakłócających pracę. Zastosowano sterowanie prądem krytycznym dla poprawy jakości pracy przekształtnika. Analizowano właściwości dynamiczne układu.* ***Sterowanie prądem krytycznym C^3 w przekształtniku z korekcją współczynnika mocy stosowanym do zasilania diod LED***

Keywords: power factor correction, LED driver, buck converter, small signal model.
Słowa kluczowe: przekształtnik buck, współczynnik mocy, zasilanie diod LED.

Introduction

Today's rapid improvement in material and manufacture methods has enabled significant developments in high luminance LED's for lighting applications. LED lamps have a wide range of operating temperature and work with low voltages and don't require to any ignition circuit comparing with fluorescent lamps [1].

The harmonic contents of the converter input current are harmful for the other electrical equipments [2]. In order to ameliorate this draw back, a power factor correction (PFC) circuit must be attached or intermixed to the converter configuration. In the PF corrected condition, input current and voltage of the converter are sinusoidal and have same phase along with each other. For simplifying the driver circuit and its cost, some single stage schemes have been proposed to perform both functions of the PFC and driving.

During the last decades, modelling and design techniques of switch mode power supplies have obtained a lot of attention. For many applications, switching converters play a primary role to produce the desired voltage condition such as LED drivers. Power stages of PWM converters are highly nonlinear systems because they contain at least one transistor and diode, which operate as switches [3]. In the recent works, switching converters are considered from an energy storage modelling point of view. The modelling techniques help to design the converter circuit more precisely and to prevent the money wasting due to trail and error repetitions [4]. Buck converters can be remarkably efficient such 95% or higher for integrated circuits, making them useful for tasks such as LED drivers, computer processor and other step downed voltage applications [2]. The converters normally require control circuits to regulate the dc output voltage against load and line variations. Typical control aspects of interest are frequency response, transient response, and stability. Linear control theory is well developed and may offer valuable tools for studying the dynamic performance of PWM converters. In order to apply this theory, nonlinear power stages of PWM converters should be averaged and linearized [5].

The Lagrange equation was first developed in 1750's by Euler and Lagrange (EL) in connection with their studies of the tautochrone problem. In Lagrange mechanics the evolution of a physical system is described by the solutions to EL equation activity of the system. This method has the advantage that it takes the same form in any generalized coordination comparing with Newton's low [6]. The electrical systems are analogous to mechanical systems; then one can apply the EL equation on them in the similar way [7].

This paper proposes a buck derived LED driver with improved power factor using critical current control (C^3) technique, then models it by Lagrange energy equation. The Lagrange model gives designer better intuition about the circuit under study. In spite of other works that consider the switch network ideal, this work joins the parasitic elements of the switch network into modelling process. The dependent sources are used to model the ideal switching network and law of energy conservation is used to model the transistor internal resistance, diode offset voltage and its resistance. After replacing the switching network with Lagrange model, a small signal model of the entire power stage is obtained. The theoretical predictions are tested and validated by means of PSIM software. PSIM software offers efficient and skilful tools to simulate the linear and nonlinear analog circuits. Finally, the precise agreement between the proposed model and simulation results has achieved.

Buck converter and Lagrange modelling

Usual buck converter scheme is presented in Fig.1.

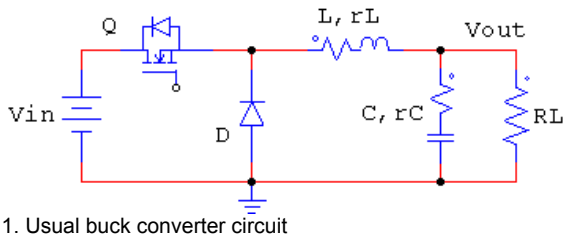

Fig.1. Usual buck converter circuit

The Lagrange differential equations provide the suitable dynamic description by including voltage source as external forces and Raleigh dissipation terms to include resistive elements [6]. In the other hand, the traditional state-space averaging (SSA) method requires considerable matrix algebra manipulation and is so tedious. Also, SSA method doesn't give any intuition about the converter under study. Lagrange equality of a non-conservative system can be defined by the following equations [8].

$$(1) \qquad \frac{d}{dt}\left(\frac{\partial \ell(q,\dot{q})}{\partial \dot{q}}\right) - \frac{\partial \ell(q,\dot{q})}{\partial q} = -\frac{\partial \psi(\dot{q})}{\partial \dot{q}} + \chi(q)\lambda + F_q$$

(2) $$\ell(q,\dot{q}) = \tau(q,\dot{q}) - \nu(q,\dot{q}) \quad , \quad \chi(q)\dot{q}^T = 0$$

In the above equations, q represents the electrical charge and q' denotes the electrical current. The scalar function of ℓ is the lagrangian operator of system that is equal to the difference between the kinetic energy (denoted by τ(q,q')) and potential one (denoted by υ(q,q')) of the system. Symbol ψ(q') is the Raleigh dissipation function of the system and the vector F_q represents the forcing function associated with each state variable coordinate. Letter λ is the intermediate variable and χ introduces the constrain forces matrix that is normally can be defined by Kirchhoff current law [8], [9].

In the proceeding discussions, d(t) symbol states the transistor on/off function and can be specified as the following equation, where T and D are switching period and duty ratio respectively, t_k represents a sampling instant.

(3) $$d(t) = \begin{cases} 1, & for \;\; t_k \le t \le t_k + D.T \\ 0, & for \;\; t_k + D.T \le t \le t_k + T \end{cases}$$
$$; \; t_{k+1} = t_k + T \;\; ; k = 0,1,2,....$$

First suppose that the transistor is on or d(t)=1, in this case the EL quantities are readily found to be:

(4) $$\tau_1(q,\dot{q}) = \frac{1}{2} L \; \dot{q}_L^2 \;\; ; \;\; \upsilon_1(q,\dot{q}) = \frac{1}{2}\frac{q_C^2}{C}$$

(5) $$\ell_1(q,\dot{q}) = \tau_1(q,\dot{q}) - \upsilon_1(q,\dot{q}) = \frac{1}{2} L \; \dot{q}_L^2 - \frac{1}{2}\frac{q_C^2}{C}$$

(6) $$\psi_1(q) = \frac{1}{2} r_T \dot{q}_L^2 + \frac{1}{2} r_L \dot{q}_L^2 + \frac{1}{2} r_C \dot{q}_C^2 + \frac{1}{2} R(\dot{q}_L - \dot{q}_C)^2$$

(7) $$F_{qL}^1 = E \;\; ; \;\; F_{qC}^1 = 0$$

r_T, r_L and r_C are the equivalent series resistors of transistor, inductor and capacitor respectively. Similarly, one can derive the EL quantities when the diode is on or d(t)=0 where are stated below:

(8) $$\tau_0(q,\dot{q}) = \frac{1}{2} L \; \dot{q}_L^2 \;\; ; \;\; \upsilon_0(q,\dot{q}) = \frac{1}{2}\frac{q_C^2}{C}$$

(9) $$\ell_0(q,\dot{q}) = \tau_0(q,\dot{q}) - \upsilon_0(q,\dot{q}) = \frac{1}{2} L \; \dot{q}_L^2 - \frac{1}{2}\frac{q_C^2}{C}$$

(10) $$\psi_0(q) = \frac{1}{2} r_T \dot{q}_L^2 + \frac{1}{2} r_L \dot{q}_L^2 + \frac{1}{2} r_C \dot{q}_C^2 + \frac{1}{2} R(\dot{q}_L - \dot{q}_C)^2$$

(11) $$F_{qL}^0 = E \; ; \; F_{qC}^0 = 0$$

By averaging the equations of (4)-(7) with (8)-(11), one can present the state equation of this system as below:

(12) $$X = [x_1, x_2] = [i_L, v_C] = [\dot{q}_L, \frac{q_C}{C}]$$
$$\dot{X} = AX + BU \;\; ; \; Y = CX + DU$$

(13) $$\begin{bmatrix} \dot{x}_1 \\ \dot{x}_2 \end{bmatrix} = \begin{bmatrix} -\frac{r + r_C}{L_1} & \frac{r_C}{L_1} \\ \frac{1}{C} & -\frac{R + r_C}{L_2} \end{bmatrix} \begin{bmatrix} x_1 \\ x_2 \\ x_3 \end{bmatrix} + \begin{bmatrix} \frac{d}{L_1} & -\frac{1-d}{L_1} \\ 0 & 0 \end{bmatrix} \begin{bmatrix} E \\ 0 \end{bmatrix}$$

Where r is the sum of inductor and transistor resistors or $r = r_L + r_T$ .Then by solving the state equation in the s-domain one can extract the dynamic transfer functions of the output voltage respect to other key variables where are presented in formulas (14) to (18).

(14) $$Y(s) = \left[C(SI - A)^{-1} B + D\right] X(s)$$

(15) $$G_v(s) = \frac{v_o(s)}{v_i(s)} = d. \frac{1 + \frac{s}{\omega_{zc}}}{1 + \frac{s}{Q\omega_o} + \frac{s^2}{\omega_o^2}}$$

(16) $$G_d(s) = \frac{v_o(s)}{d(s)} = V_I. \frac{1 + \frac{s}{\omega_{zc}}}{1 + \frac{s}{Q\omega_o} + \frac{s^2}{\omega_o^2}}$$

(17) $$Z_o(s) = \frac{v_o(s)}{i_o(s)} = (R \,||\, r). \frac{(1 + \frac{s}{\omega_{zc}})(1 + \frac{s}{\omega_{zl}})}{1 + \frac{s}{Q\omega_o} + \frac{s^2}{\omega_o^2}}$$

(18) $$\omega_o = \frac{1}{\sqrt{LC}} ; \; \omega_{zc} = \frac{1}{r_C.C} ; \omega_{zl} = \frac{r}{L} ; \; Q = \frac{R}{\sqrt{\frac{L}{C}}}$$

Where, G_v is the audio-success-ability transfer function, G_d is control-to-output ratio [10] and Z_o is the equivalent impedance seen from converter output. One can define and derive the arbitrary transfer functions between the system parameters. The main triple functions are shown in Fig. 2.

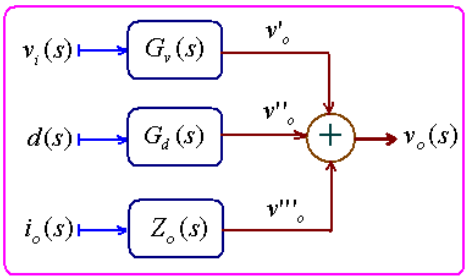

Fig.2. Open-loop functional block of the converter in s-domain

Numerical example of buck converter Lagrange model

This section presents the proposed Lagrange model of an instantaneous buck converter to better demonstrate the accuracy and precision of the suggested approach.

First consider the converter shown in Figure 1 with the values stated in Table.1.

Table1. The buck converter components value

Converter parts value	
Part	Value
V_{in}	100V
L , r_L	2mH , 0.1Ω
C , r_C	220uF ,0.05Ω
R_L	25Ω
D ratio	0.5
r_T	0.1Ω
V_F	0.5V

Using equation (18) and table1 one can define the converter quality factor and other main frequencies as:

(19) $$\omega_o = 1.5k \, rad/\sec ; \; \omega_{zc} = 90k \, rad/\sec ;$$
$$\omega_{zl} = 50 \, rad/\sec \;\; ; Q = 8.2$$

Figure 3 for example, shows the audio-success-ability transfer function of the given converter. Circuit simulation result is denoted by phrase "sim" and modelling one is

denoted by "mdl". Amplitude and phase axis units are decibel and degree respectively. Phase margin (PM) and gain margin (GM) are about -70^{o} and -30db respectively.

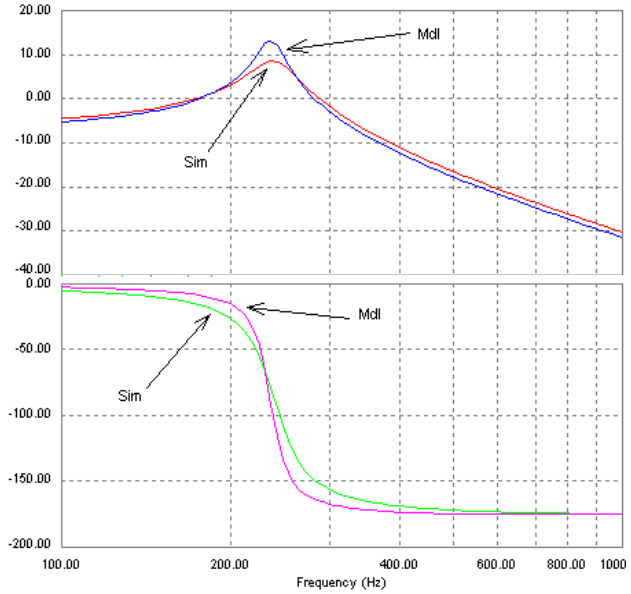

Fig.3. simulation and modelling results of the given converter audio-success-ability transfer function; amplitude (top), phase (bot)

To determine the influence of system input variable where shown in fig. 2 on the converter output voltage, it is sufficient to apply the inverse laplacian operator on the s-domain corresponding function. Fig.4 depicts the converter output voltage when starts up. Converter start-up behaviour can be supposed such as applying the step change with 100V amplitude on the converter input source (V_{in}).

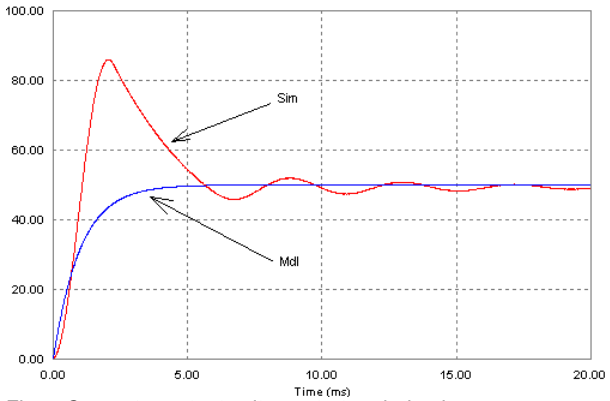

Fig.4. Converter output voltage start-up behaviour

The figure below, shows the converter input current.

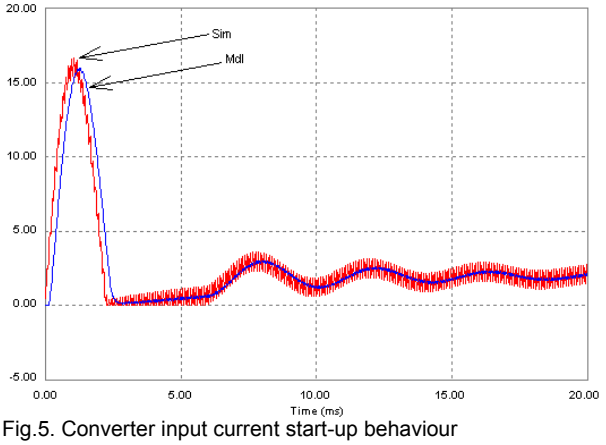

Fig.5. Converter input current start-up behaviour

C^3 technique applied on PFC buck based LED driver

This section presents a power factor corrected buck converter witch is used as a LED driver. Its control loop mechanism is found on the critical current control (C^3) method. Converter parts value is the same as in table 1. Closed loop converter scheme is shown in figure 6.

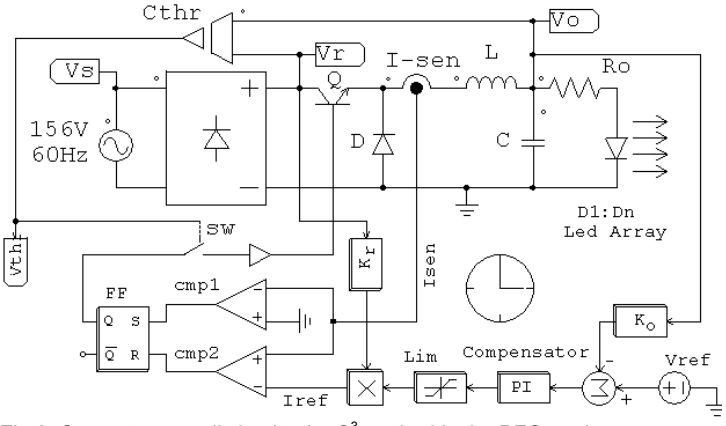

Fig.6. Converter overall circuitry by C^3 method in the PFC mode

This converter has two loops: an inner current loop and outer voltage loop. The inner loop contains a current sensor, two op-amp comparators and a set-reset latch. Current sensor can be modelled as a resistor (R_s) witch convert the sensed current to the voltage applied to op-amp's input leads [11]. Outer loop consists of a voltage comparator, a PI compensator, an error limiter and one multiplier. Voltage comparator (Σ) compares the converter output voltage with desired reference voltage (V_{ref}), and then yielded error feeds the PI block input error. Afterward, limiter clips the compensated error to prevent the unwanted bounces. Output voltage loop compensator modulates the reference current amplitude (I_{ref}) using a multiplier block.

I_{ref} amplitude indicates the demanded power of output LED lamps. In the buck converter, power flows from source to load only when the input voltage is grater than output voltage due to its electrical structure where is seen in Fig.7.

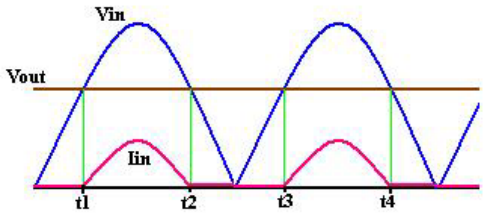

Fig.7. Buck converter input current flows only when $V_{in} > V_{out}$

C^3 technique also called borderline conduction mode (BCM) offers numerous advantages. Control circuit detects the moment at witch the inductor current reaches zero then sets the switch on, also resets it when the inductor current reaches to the upper reference value (I_{ref}). Due to this specification, switch sets on when the current is zero or the zero current switching (ZCS) state occurs, also no reverse recovery effects bother the designer even in short circuit and start-up sequences. Since the converter stays between CCM and DCM, it is possible to approximate its response with first order system, easing the procedure to design the closed loop feedback [11], [12].

C^3 technique operates without an internal clock and the switching frequency is naturally dependent on the external conditions to compel the converter to operate between CCM and DCM boundary. The delay time (t_d) introduced by power transistors driver and pulse width modulator can be described by the delay function of $H_d(s)$ witch is valid from 0

Hz (DC) upto the half of switching frequency ($F_s/2$) that is approximated in the following formula [3], [13].

$$H_d(s) = e^{-st_d} = \frac{1-\frac{st_d}{2}}{1+\frac{st_d}{2}} = \frac{s-\frac{2}{t_d}}{s+\frac{2}{t_d}} = \frac{s-\omega_y}{s+\omega_y}; \omega_y = \frac{2}{t_d} \quad (20)$$

Simulation and proposed modelling method results

Source current and output voltage are depicted in Fig.8. As seen, source current has the sinusoidal shape inphase with its voltage and flows only when the input voltage amplitude exceeds the output voltage level. Modelling result stays on the instantaneous average value of source current.

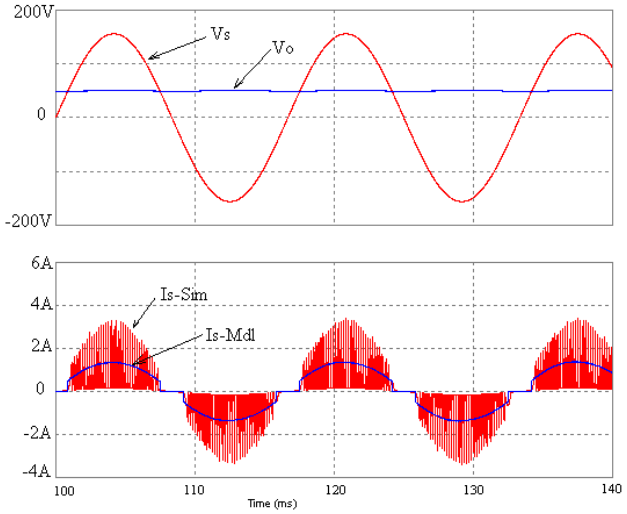

Fig.8. Converter source current and voltage along with each other

Similarly, Figure 9 shows the reference current, input voltage and current of converter after the diode bridge.

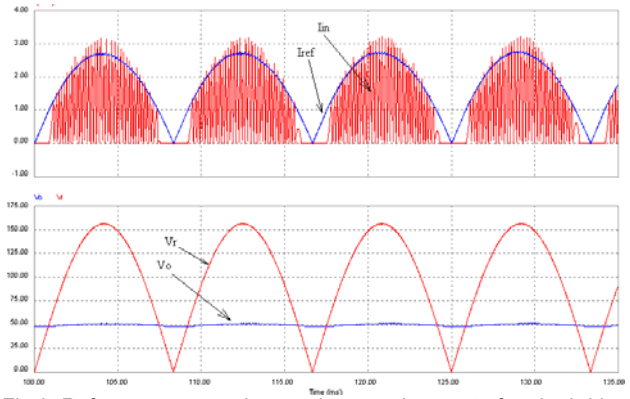

Fig.9. Reference current, input voltage and current after the bridge

Figure 10, shows frequency content of the input current.

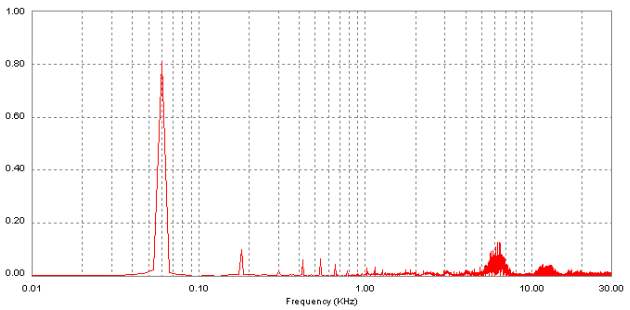

Fig.10. Harmonic contents of the converter input current

According to this curve, total harmonic distortion factor (THD) of the input current is about 96%; also Y-axis is scaled in per-unit (PU). The following figure compares the output voltage at the start-up time provided by simulation and proposed modelling technique.

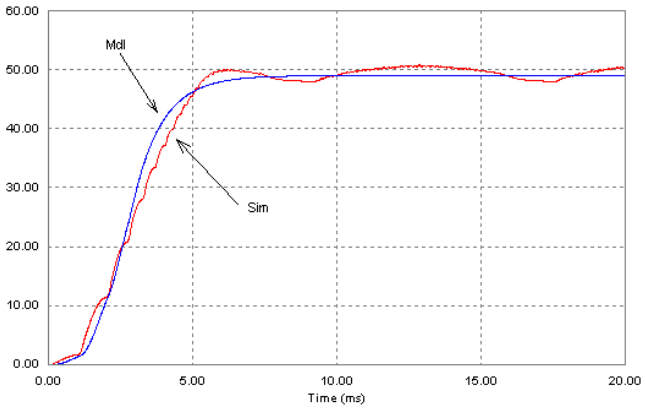

Fig.11. Output voltage at the start-up moment

Output capacitor value is a main factor that defines the output voltage ripples witch must be limited below an acceptable value. Capacitor current helps the designer to select its value correctly where is depicted in figure 12.

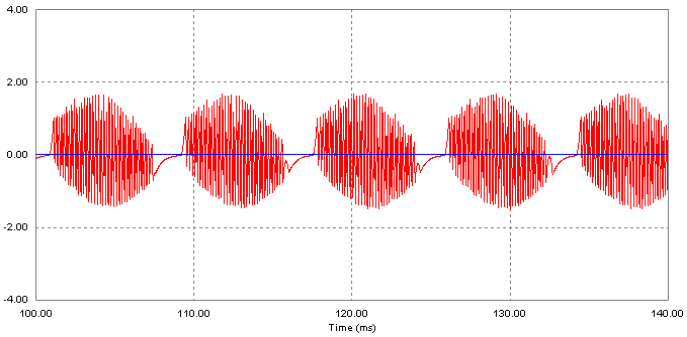

Fig.12. Output capacitor current

To determine the influence of step change of any input variables on the converter output voltage, it is sufficient to multiply the corresponding transfer function by the changed amplitude value in the s-domain as stated by the following formulas [3]. Phrase 'ℓ^{-1}' denotes inverse laplacian operator.

$$\Delta v_o(t) = \ell^{-1}\left(\frac{G_V}{1+T}.\Delta v_i\right) \quad (21)$$

$$\Delta v_o(t) = \ell^{-1}\left(\frac{G_d}{1+T}.\Delta v_r\right) \quad (22)$$

$$\Delta v_o(t) = \ell^{-1}\left(-\frac{Z_P}{1+T}.\Delta i_o\right) \quad (23)$$

Figure 13, shows the converter input current when the output load consumption is doubled deliberately.

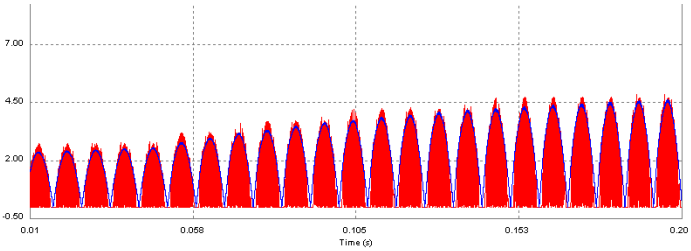

Fig.13. Load change effect on the converter input current

Conclusion

This paper analyses a buck based LED driver with improved power factor. Power factor correction is done using critical current control (C^3) or borderline conduction mode (BCM). Also, the Lagrange differential equations are employed here as an efficient tool for switching converter modelling in the closed loop condition. The proposed modelling technique gives the designer better intuition about the circuit under study rather than traditional state-space averaging (SSA) method. SSA is a tedious and fully mathematical tool for switching converters modelling.

In addition, parasitic elements of the converter have taken into account so it helps to select the circuit parts value correctly before manufacturing process.

Dynamic behaviour of the converter is analysed in both frequency and time domain such as transfer functions and step response. A PI compensator is employed in the closed feedback loop to stabilize and modulate the reference current amplitude corresponding to the demanded power. Since this method relying on the averaging method, then the final model is reliable from 0 Hz up to half of switching frequency according to the Nyquist theorem.

Finally, the simulation results confirm the proposed model exactness and indicate the rapidity of system step response under compelling conditions.

REFERENCES

[1] Jardini J.A. et al., Power Flow Control in the Converters Interconnecting AC-DC Meshed Systems, *Przegląd Elektrotechniczny,* 01(2015), 46-49.

[2] Gajowik T., Rafał K., Bobrowska M., Bi-directional DC-DC converter in three-phase Dual Active Bridge Topology, *Przegląd Elektrotechniczny*, 05(2014), 14-20.

[3] Kazmierczuk M.K., Pulse Width Modulated DC-DC Power Converters, Wiley, Ohio, 2008.

[4] Ben-Yaakov S., Average simulation of PWM converters by direct implementation of behavioural relationships, *IEEE Conf. , APEC,* 1993, San diego, CA., 510-516.

[5] Shepherd W., Zhang L., Power Converter Circuits, Marcel & Dekker Inc., New York, 2004.

[6] Curry J., Hamiltonian and Lagrangian Mechanics, Vol.1, Ed.2, CSI Publishing, USA, 2013.

[7] Hand L.N., Finch J.D., Analytical Mechanics, Camb. Univ. Press, UK, 1999.

[8] Ramirez S.H. et al., Passivity-Based Control of Euler-Lagrange Systems, Springer, London, 1998.

[9] Scherpen J.M.A., Jeltsema D., Klaassens J.B., Lagrangian modelling of switching electrical network, *Systems and control letters,* 48(2003), 365-374.

[10] Joseph N., Control and Analysis of Synchronous Rectifier Buck Converter for ZVS in Light Load Condition, International Journal of Advanced Research in Electrical, *Electronics and Instrumentation Engineering,* 02(2013), No. 06, 2440-2447.

[11] Kursun V., Narendra S., Vivek K., Friedman G., Efficiency Analysis of a High Frequency Buck Converter for On-Chip Integration with a Dual-VDD Microprocessor, *ESSCIRC*, 2002, 743-746.

[12] Zdanowski M., Rąbkowski J., Barlik R., High frequency DC/DC converter with Silicon Carbide devices - simulation analysis, *Przegląd Elektrotechniczny*, 02(2014), 201-205.

[13] Basso P., Switch mode power supplies, McGraw-Hill, 2008.

Authors

A. Skandarnezhad, a_skandarnezhad@iust.ac.ir
PhD student, Electrical engineering, Faculty of Electrical Engineering, Iran University of Science and Technology (IUST), Tehran, Iran.

A. Rahmati, rahmati@iust.ac.ir
Associated professor, Electrical engineering, Faculty of Electrical Engineering, Iran University of Science and Technology (IUST), Tehran, Iran

A. Abrishamifar, abrishamifar@iust.ac.ir
Associated professor, Electrical engineering, Faculty of Electrical Engineering, Iran University of Science and Technology (IUST), Tehran, Iran

S. Shahmohammadi, s_shahmohammadi@iust.ac.ir
PhD student, Electrical engineering, Faculty of Electrical Engineering, Iran University of Science and Technology (IUST), Tehran, Iran.

* The corresponding author email address is:
a_skandarnezhad@iust.ac.ir